

Formulation of ceramic foams

Celani, Andrea; Blackburn, Stuart; Simmons, Mark; Holt, Liz M.; Stitt, E. Hugh

DOI:

[10.1016/j.colsurfa.2017.07.031](https://doi.org/10.1016/j.colsurfa.2017.07.031)

License:

Creative Commons: Attribution (CC BY)

Document Version

Publisher's PDF, also known as Version of record

Citation for published version (Harvard):

Celani, A, Blackburn, S, Simmons, M, Holt, LM & Stitt, EH 2018, 'Formulation of ceramic foams: a new class of amphiphiles', *Colloids and Surfaces A: Physicochemical and Engineering Aspects*, vol. 536, pp. 104-112.
<https://doi.org/10.1016/j.colsurfa.2017.07.031>

[Link to publication on Research at Birmingham portal](#)

General rights

Unless a licence is specified above, all rights (including copyright and moral rights) in this document are retained by the authors and/or the copyright holders. The express permission of the copyright holder must be obtained for any use of this material other than for purposes permitted by law.

- Users may freely distribute the URL that is used to identify this publication.
- Users may download and/or print one copy of the publication from the University of Birmingham research portal for the purpose of private study or non-commercial research.
- User may use extracts from the document in line with the concept of 'fair dealing' under the Copyright, Designs and Patents Act 1988 (?)
- Users may not further distribute the material nor use it for the purposes of commercial gain.

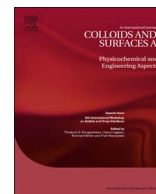
Where a licence is displayed above, please note the terms and conditions of the licence govern your use of this document.

When citing, please reference the published version.

Take down policy

While the University of Birmingham exercises care and attention in making items available there are rare occasions when an item has been uploaded in error or has been deemed to be commercially or otherwise sensitive.

If you believe that this is the case for this document, please contact UBIRA@lists.bham.ac.uk providing details and we will remove access to the work immediately and investigate.



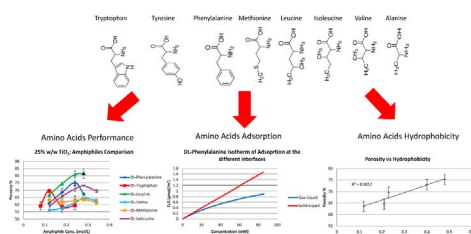
Formulation of Ceramic Foams: a New Class of Amphiphiles

Andrea Celani^{a,b,*}, Stuart Blackburn^a, Mark J. Simmons^a, Liz M. Holt^b, E. Hugh Stitt^b

^a School of Chemical Engineering, University of Birmingham, B15 2TT, United Kingdom

^b Johnson Matthey Technology Centre, Billingham, TS23 1LB, United Kingdom

GRAPHICAL ABSTRACT



ARTICLE INFO

Keywords:

Ceramic Foams
Amino Acids
Hydrophobicity
Isotherm of Adsorption

ABSTRACT

In this work, amino acids are proposed and assessed as a new class of amphiphiles that is more environmentally benign and present a wider operational window than those reported in the literature. The effects of the amphiphile concentration and structure on the foam properties were investigated (e.g. porosity, bubble size distribution). These were classified depending on their different hydrophobicity by establishing a hydrophobicity index. Monotonic relationships between the hydrophobicity index and the foam structural properties (e.g. porosity, bubble size) were found. In addition, the more suitable amino acid to be used at larger scales was identified and it was used as a model amphiphile to have a deeper insight into the foaming process. In particular, the repartition of the amino acids among the different interfaces and the minimum amphiphile concentration to obtain stable foams were identified.

1. Introduction

In recent years ceramic foams have been receiving an increasing interest thanks to their applicability in several technology fields. Among others, ceramic porous materials are used as refractory insulators, catalyst supports and filters for molten metals [1,2]. Several techniques have been developed for the production of ceramic foams; these include replica technique, sacrificial templating and direct foaming [3]. The replica technique consists in the impregnation of a natural (e.g. wood [4], coral [5]) or a synthetic template (e.g. polymer foam [6]) with a ceramic suspension. In order to obtain a thin ceramic coating on the template surface, the suspension in excess is removed by passing the template through rollers. After drying and calcination a

ceramic positive replica of the template is obtained. Sacrificial templating uses a biphasic mixture of a template and ceramic slurry to generate the porous structure inside the ceramic body. The sacrificial material can be natural [7] or synthetic [8] and either in solid [9] or liquid form [10]. These are then either extracted or decomposed to form a negative replica of the sacrificial template in the ceramic material. Direct foaming is an ostensibly straightforward method for the production of ceramic foams. In this process, air is directly entrained into the ceramic suspension causing the attachment of the previously modified particles at the air/water interface, leading to stable foams [11]. Particles surface properties are modified in order to reduce their hydrophilicity. This is realized through the addition of an amphiphile; namely a chemical that has a polar head which electrostatically

* Corresponding author at: School of Chemical Engineering, University of Birmingham, B15 2TT, United Kingdom.
E-mail address: andrea.celani@matthey.com (A. Celani).

interacts with the particles surface and a hydrophobic tail that is directed toward the aqueous phase. Several classes of chemicals have been proposed as amphiphiles, these include among others carboxylic acids, amines and gallates [11]. The selection of the suitable amphiphile is largely governed by the particle's surface charge where carboxylic acids are used with positively charged particles, amines with negatively charged particles and gallates with either positively charged or neutral particles. It has been demonstrated that both the structural characteristics of the amphiphile and its concentration strongly affect foam properties such as porosity, stability and bubble size distribution [12,13].

Although the use of the previously mentioned amphiphiles is widely reported in the literature, the use of these amphiphiles is limited to a certain pH range dictated by the particle surface charge. In addition, many of these amphiphiles present acute toxicity limiting their usage at production scale. The aim of this work is to investigate the possibility of using amino acids as amphiphiles. Amino acids are organic compounds containing an amine group ($-\text{NH}_2$), a carboxylic group ($-\text{COOH}$) and a side chain specific to each amino acid. There are about 500 natural occurring amino acids [14]; these can be classified according to the position of the functional groups in alpha- (α), beta- (β), gamma- (γ) or delta- (δ). In this work attention was posed on the alpha- amino acids; in these molecules the carboxylic and the amino groups are attached to the first carbon or alpha- (α) carbon. The selection of this class of amino acids was based on their lower cost relative to hydrophobic β -, γ - and δ -amino acids making them more economically suitable for the scale up of the process in the future. This class of molecules is environmentally friendly and allows a wider pH operational window courtesy of the presence of both the carboxylic and the amino group on the same molecule. In the present study the amino acids are classified according to their different hydrophobicity. This is then shown to influence both the porosity and the bubble size distribution of the obtained foams. Among the tested amino acids the best amphiphile in term of operability is identified; then its adsorption at the different interfaces and the minimum amphiphile concentration necessary to obtain stable foams is identified.

2. Materials and Methods

2.1. Materials

Fumed TiO_2 particles (grade AEROXIDE P25) were obtained from Evonik Industries (Essen, Germany). The supplier technical data sheet states that the primary particles have a mean diameter of approximately 21 nm while their aggregates are several hundred nm in size. Density and surface area are 4 g/cm^3 and $50 \text{ m}^2/\text{g}$ respectively. The AEROXIDE P25 is characterised by an anatase/rutile ratio of 80/20 with both crystal structures having a tetragonal geometry.

The amino acids used to modify the particles surface were DL-Alanine 99%, DL-Valine 99%, DL-Isoleucine 99%, DL-Leucine 99%, DL-Methionine 99%, DL-Phenylalanine 99%, DL-Tyrosine 98% and DL-Tryptophan 99% (Alfa Aesar, Heysham, United Kingdom). Other chemical used in the experiments were demineralised water, nitric acid 70% v/v (Alfa Aesar, Heysham, United Kingdom) and potassium hydroxide solution 40% v/v prepared by dissolving potassium hydroxide pellets (Alfa Aesar, Heysham, United Kingdom) in demineralised water.

2.2. Suspension Preparation

Titania suspensions were prepared by stepwise addition of the powder to deionised water continuously stirred using an IKA EUROSTAR power control-visc overhead mixer. The pH of all suspensions was adjusted to electrostatically stabilise the particles. Titania particles are stable at pH either below 4 or above 7. To favour the dissolution of amino acids the pH was kept either below 2 or above 10 through the addition of small aliquots of 70% v/v HNO_3 and 40% v/v

KOH respectively. The solid loading of titania suspensions was set to 25% w/w. In a typical formulation, carried out at acid pH, 99.7 g of titania was added to 250 ml of demineralised water containing 50 ml of 5% v/v HNO_3 . After powder dispersion the suspension pH was dropped below 2 through the addition of 5 ml of 70% v/v HNO_3 . Then an amino acid was added to the titania suspension to obtain the required concentration in the range 0.08 and 0.36 mol/L.

2.3. Foaming and Foam Characterisation

Foaming of 300 mL suspension was carried out using an overhead stirrer equipped with a gas inducing impeller [15]. The vessel diameter and impeller diameter were $T = 12 \text{ cm}$ and $D = 6 \text{ cm}$ respectively ($D/T = 50\%$). The vessel was fitted with 4 baffles 1 cm wide ($B/T = 8.3\%$). Mixing was carried out at 2000 rpm for 20 minutes. The foam was dried under ambient conditions and then calcined in a Carbolite Furnace CWF at 600°C for 4 hours. During the ramping step and for the first 45 minutes the furnace was purged under N_2 followed by air. The heating rate was 2°C/min .

The porosity of the calcined foam was initially evaluated by both mercury intrusion porosimetry and water pick-up. The average difference between the two techniques was 4% so the quicker water pick-up experiment was used for further analysis; for this reason, only the porosity values determined by water pick-up are reported herein. In this technique, the initial weight of four foam samples was recorded then these were immersed in water and the weight of the wetted samples was recorded over a four days period. The average amount of water picked up was determined by difference between the weight of the wet foam and the initial weight. From this value the foam porosity and pore volume were calculated.

Foam bubble size distribution was determined by acquiring optical microscope (Nikon Eclipse E200) images of the foam cross section. Bubble's diameters were obtained by analysing the acquired images with Fiji ImageJ 1.50a (Wayne Rasband, National Institute of Health, USA) [16]. The obtained diameters were corrected by dividing them by 0.79 in order to take into account the random position of the bubbles during sample sectioning. The correction factor was determined by Williams et al.; they identified that the mean pore diameter determined from 2D images is 79% of the actual pore diameter. This factor was derived from numerical methods that they developed and described in order to correct the underestimated pore size obtained from 2-D cross section [17].

2.4. SS-NMR

Titania suspensions having pH of 1, 4 and 10 were prepared using the procedure described in Section 2.2. Titania particles were modified by the addition of 0.2 mol/L of DL-Phenylalanine. The suspensions were dried at ambient condition and then ground using mortar and pestle. The SS-NMR spectrum was acquired at a static magnetic field strength of 9.4 T ($\nu_0(^1\text{H}) = 400.16 \text{ MHz}$) on a Bruker Avance III console using a widebore Bruker 4 mm BB/1H WVT MAS probe and TopSpin 3.1 software. For ^{13}C , the probe was turned to 100.63 MHz and the spectrum referenced to the alanine CH_3 signal at 20.5 ppm. The powdered sample was packed into a zirconia MAS rotor with a Kel-F cap, with weighing before and after packing to obtain the sample mass. The rotor was spun using room-temperature purified compressed air. The total experiment time to acquire the spectrum was 18 hours. The spectrum was acquired using the cross polarisation (CP) method, in which magnetisation on ^1H nuclei is transferred to nearby ^{13}C nuclei via the dipolar coupling. Magnetisation was transferred in a contact time of 1 ms. High power (100 W) SPINAL-64 decoupling was applied to the ^1H channel during acquisition.

2.5. Surface Tension Measurements

The surface tension of both suspensions and amino acid solutions was measured using the pendant drop method (Krüss Drop Shape Analyser, Hamburg, Germany). In this method, a drop of the solution under analysis is suspended from a needle. The shape of the drop results from the relationship between the surface tension and gravity. Using the drop shape analysis software, the solution surface tension can be determined using the following formula [18] (Eq. (1)):

$$\gamma = \frac{\Delta \rho g R^2}{\beta} \quad (1)$$

where γ is the surface tension in mN/m, $\Delta \rho$ is the density difference between the two phases in kg/m³, g is the gravitational acceleration (9.81 m/s²), R is the maximum drop radius (m) and β is the shape factor. Suspensions were prepared using the procedure mentioned in Section 2.2 while amino acid solutions were prepared dissolving different amount of amino acids in 45 ml of demineralised water containing 5 ml of 70% v/v of HNO₃. The drop volumes were in the range 20 μ L–25 μ L, depending on the surface tension of the sample. At least 5 drops for each sample were analysed in order to obtain an average value of the surface tension.

2.6. Suspension Filtration and Supernatant UV–Vis Analysis

To determine the amount of amino acid adsorbed at the particles surface, titania suspensions having different amino acid concentration were prepared. 99.6 g of titania were stepwise dispersed in 300 ml of demineralised water. Amphiphile concentrations between 0.01 M and 0.125 M were dissolved in the suspension. To favour the amphiphile–particles interaction the modified suspensions were stirred at 200 rpm for 20 minutes using an overhead stirrer. The suspensions were then centrifuged at 3000 rpm for 90 minutes using a Falcon 6/300 centrifuge (MSE, London, United Kingdom). The supernatant was then separated from the solid residue. To remove finer particles still in suspension, the supernatant was filtrated using 0.1 μ m PTFE membrane syringe filters (Whatman GE Healthcare, Amersham, United Kingdom). The filtrate was diluted ten times and the amino acid concentration was determined by UV–Vis. The UV–Vis spectra were recorded using a UV-1 ThermoSpectronic (Thermo Scientific, USA).

3. Results and Discussion

3.1. Amino Acids Screening

To assess the performance of the different amino acids, titania suspensions, prepared as described in Section 2.2, were foamed using different amino acids and amino acid concentrations; the hydrophobic amino acids used in this work are shown in Fig. 1. At pH < 2 the titania surface is positively charged due to the presence of $-\text{OH}_2^+$

groups [19]. At this conditions the dissociated fraction of $-\text{COO}^-$ groups present on the amino acids electrostatically interacts with the titania surface. The pK_a of the carboxylic group of the tested amino acids ranges between 1.8 and 2.4 and, at pH < 2, less than 20% of the carboxylic groups are dissociated but the low solubility of some of the amino acids made it necessary to work at such a low pH. The amino acid solubility is strongly dependent on the pH; Tseng et al. showed, for example, that the solubility of DL-Isoleucine is around 40 g/L at pH comprised between 3 and 8 while it is greater than 150 g/L for pH < 1.5 and pH > 10.5 [20].

Fig. 2 shows the difference in the foam structure when different amino acids are used as amphiphiles (e.g. Phenylalanine and Tryptophan respectively) while Fig. 3 reports the porosity trend of foams obtained using different amino acids and amino acid concentrations.

The lines connecting the experimental points in Fig. 3, are meant to guide the reader eyes and not to fit them. With the exception of DL-Methionine, an increase in porosity was observed increasing the amphiphile concentration till it reached a maximum value, beyond which the porosity decreased. The initial increase in porosity is due to the higher concentration of amphiphile adsorbed on the particles surface resulting in a higher particle hydrophobicity giving in turn more stable foams. A further increase in the amino acid concentration in solution however leads to saturation of the particles surface by the amphiphile. This causes a reduction in electrostatic stabilisation, that in turn increases the suspension viscosity hindering air entrainment. This trend was also observed by Gonzenbach et al. when producing ceramic foams using different concentration of amphiphiles [11]. The fact that DL-Methionine does not follow this trend suggests that the amino acid was either slightly adsorbed on the particles surface or that the particles saturation by the amphiphile was already been reached and, consequently, a further increase in the amino acid concentration did not result in an increase in particles hydrophobicity. In addition, it can be noted that different amino acids gave different values of the maximum porosity obtainable while the use of DL-Alanine and DL-Tyrosine as amphiphiles did not lead to the formation of stable foams.

3.2. SS-NMR Analysis

It was theorised that amino acids would be capable of acting as amphiphiles even in basic conditions thanks to the presence of the amino group; the protonated fraction of $-\text{NH}_3^+$ groups could, in fact, electrostatically interact with the $-\text{O}^-$ groups present on the titania surface at basic pH [19]. To confirm this hypothesis dried samples of functionalised titania were analysed by SS-NMR following the methodology reported in section 2.4. Fig. 4 shows the spectra for the samples prepared at pH = 1 (red line), at pH = 4 (green line) and at pH = 10 (blue line).

At pH = 1 less than 5% of the amino acid carboxylic group was dissociated so the particles–amphiphile interaction was assumed to be negligible. The chemical shift values relative to DL-Phenylalanine

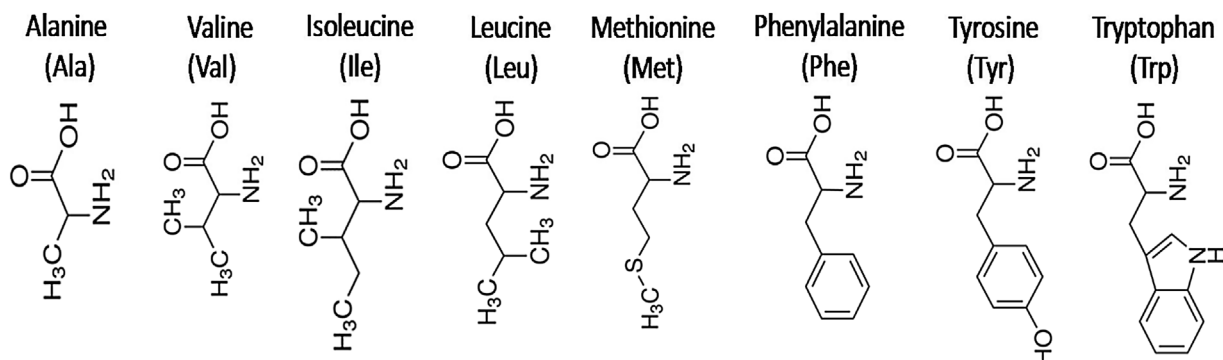


Fig. 1. Hydrophobic α -amino acids tested in this work.

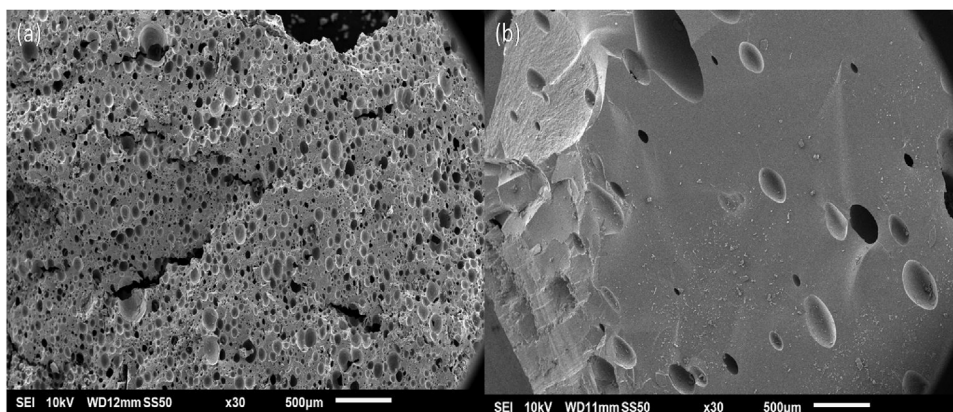


Fig. 2. SEM images of foam cross section produced using: (a) Phenylalanine and (b) Tryptophan as amphiphiles.

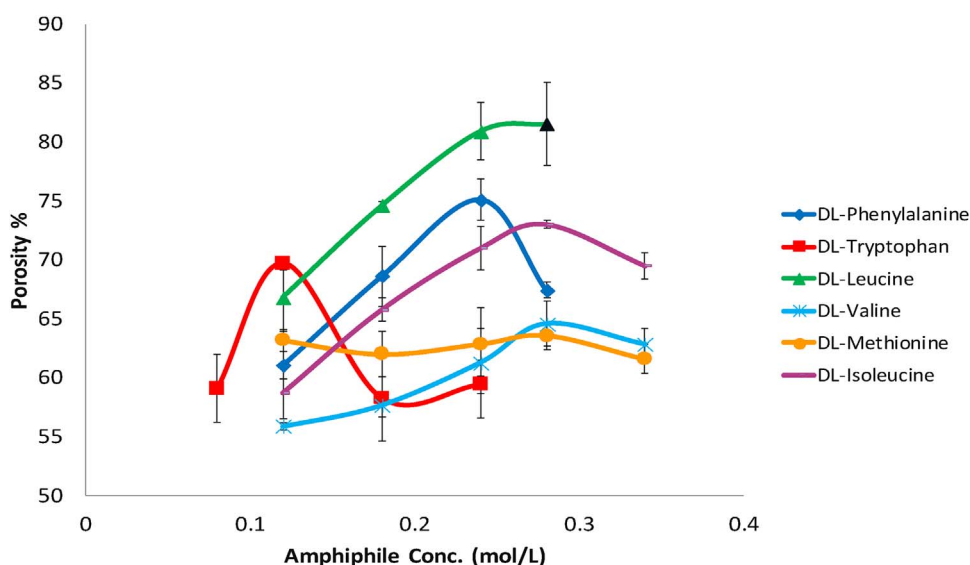


Fig. 3. Foam porosity as a function of amphiphile concentration for foams obtained using different amino acid concentrations. The black triangle in the Leucine curve indicates the solubility limit point. DL-Alanine and DL-Tyrosine are not present in the graph since they did not give stable foams.

carbons are reported next to each of them in the amino acid structure shown in Fig. 4; these were obtained from a database search and were relative to Phenylalanine in solution. It should be noted that the chemical shifts observed for the solid sample were very close to the solution data. In addition, the fact that the peaks were sharp suggested that no particle-amphiphile interaction was present. The spectrum for the solid sample prepared at pH 4 (green line) shows that the sharp peaks seen for the pH 1 solution derived sample, and attributed to crystalline Phenylalanine, are no longer present. The broadening of the carbonyl and α -carbon peaks indicates that the Phenylalanine has a more amorphous structure. The spectrum of the basic solution derived sample (blue line) shows sharp peaks for the aromatic and carbonyl sites, but peaks of the α - and β -carbons are broader. This implies a difference in the local environment of these sites, possibly a disordered distribution of environments or hindered mobility that could be an indication of an interaction between the titania and the Phenylalanine amino group. Although titania is weakly paramagnetic ($\chi_{\text{mol}} = 74 \text{ m}^3/\text{mol}$), this is probably too weak an effect to cause the observed broadening. The changes in the α - and β -carbon peaks in basic conditions and the changes in the carbonyl and α -carbons peaks in acidic conditions confirm the interaction of the amino acid through the amino and the carboxylic group in basic and acid conditions respectively. This confirms the initially suggested capability of the amino acids of interacting with both positively and negatively charged particles extending, as a consequence, the pH operating range with respect to the amphiphiles commonly reported in the literature.

3.3. Amphiphile Adsorption at the Different Interfaces

The presence of three phases (e.g. solid, liquid and gas) in the system leads to three interfaces: solid-liquid, solid-gas and liquid-gas. The relative adsorption of the amphiphile on these interfaces affects the hydrophobic character of the modified particles [21]. It will be shown later that, for several reasons, Phenylalanine presents the best choice of amphiphile from those studied in this work. It was therefore used as a representative example for the determination of the amphiphile adsorption at the different interfaces. In this work attention was posed on firstly identifying the amount of amphiphile adsorbed at the particles surface (e.g. solid-liquid interface) and consequently to determine the concentration of amino acid present as a free amphiphile in solution. Then, the amount of free amphiphile adsorbed at the liquid-gas interface was evaluated. The amount of amphiphile adsorbed at an interface can be described by an isotherm of adsorption which relates the amount of amphiphile adsorbed at the interface Γ to its bulk concentration c [22]. One of the most commonly used non-linear isotherms is that of Langmuir (Eq. (2)) [23].

$$\Gamma = \Gamma_{\text{max}} \frac{c}{c + a} \quad (2)$$

where a is the Langmuir constant [24] and Γ_{max} the maximum concentration of adsorbed amphiphile. The Langmuir isotherm is based on a lattice-type model with the assumptions that every adsorption site is equivalent (same energy of adsorption) and that the probability for adsorption at an empty site is independent of the occupancy of

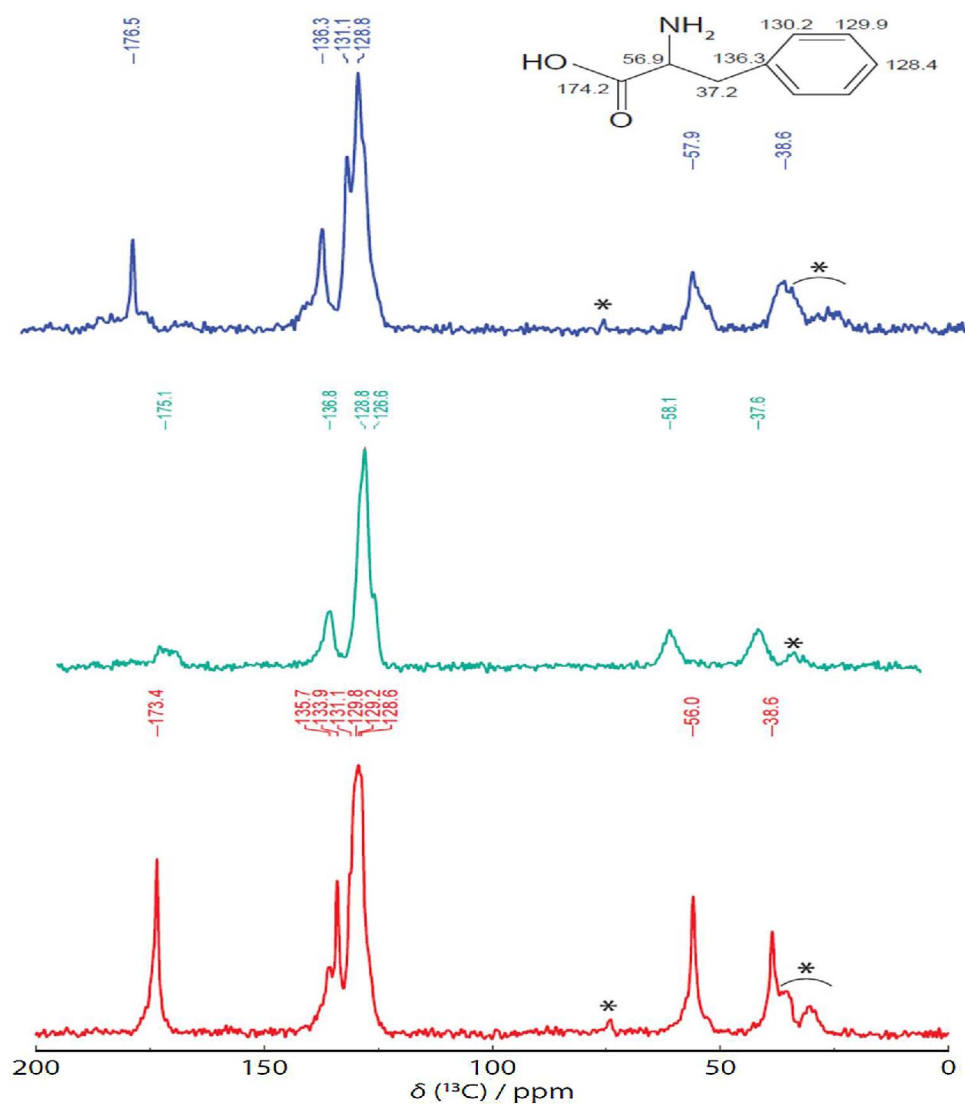


Fig. 4. SS-NMR spectra for the samples prepared at pH = 1 (red line), pH = 4 (green line) and pH = 10 (blue line).

neighbouring sites, that there are no interactions between the monomers and that no intermolecular forces act between the latter [25]. The adsorbed amount of amphiphile at the solid-liquid Γ_{SL} and gas-liquid Γ_{GL} interfaces could not be directly measured. Firstly, the adsorption of amphiphile at the particles surface Γ_{SL} was determined by differential concentration determination of the amino acid in the supernatant of particulate suspensions, before and after some equilibrating time as described in section 2.6. The adsorption at the gas-liquid interface Γ_{LG} was obtained from the surface tension γ of Phenylalanine solutions, having different concentrations, using the Langmuir-Szyszkowsky's state equation [26] (Eq. (3)), which relates the equilibrium interfacial tension to the bulk amphiphile concentration c .

$$\gamma = \gamma_0 - RT\Gamma_{\max} \ln \left(1 + \frac{c}{a} \right) \quad (3)$$

where γ_0 is the interfacial tension corresponding to the amino acid free interface and R and T are the gas constant and temperature respectively. The result, in Fig. 5, confirms that there is a progressive decrease in the surface tension with rising concentration of the amino acid. This indicates the effective adsorption at the air liquid interface. From Fig. 5 it can be noted the absence of the plateau indicative of the critical micelle concentration (C.M.C.); this is due to the low solubility of phenylalanine at pH 4.

Fitting these data with the Langmuir-Szyszkowski equation allowed the values of Γ_{\max} and a to be determined. Table 1 summarises the Γ_{\max}

and a values for both the solid-liquid and the gas-liquid interfaces.

These values were then substituted into the Langmuir isotherm equation for each amphiphile concentration giving the amount of amino acid adsorbed at the liquid-gas interface. Fig. 6 shows both the isotherm of adsorption at the solid-liquid and gas-liquid interfaces.

Comparing the isotherms at the two different interfaces (Fig. 6) it is possible to observe the preferential adsorption of the amphiphile on one interface or the other. At Phenylalanine concentrations below 10 mM the amphiphile is equally distributed between the two interfaces while at higher concentrations the amino acid preferentially adsorbs at the solid-liquid interface with this trend more and more pronounced as the concentration increases. In Fig. 6 it can be observed that the gas-liquid isotherm starts to reach a plateau corresponding to the saturation of the considered interface. The same trend cannot be observed for the solid-liquid isotherm since the solubility limit for the amino acid was reached before particles surface saturation.

3.4. Amino Acids Hydrophobicity

The measurement of surface tension of amino acid solutions has been employed to rank them based on their hydrophobicity [27]; Bull et al. [25] showed that the gradient of the surface tension curve constitutes a hydrophobicity scale for the amino acids. Specifically, it was noted that the higher the gradient the higher the hydrophobicity. Although it was commented that expressing the hydrophobicity index in

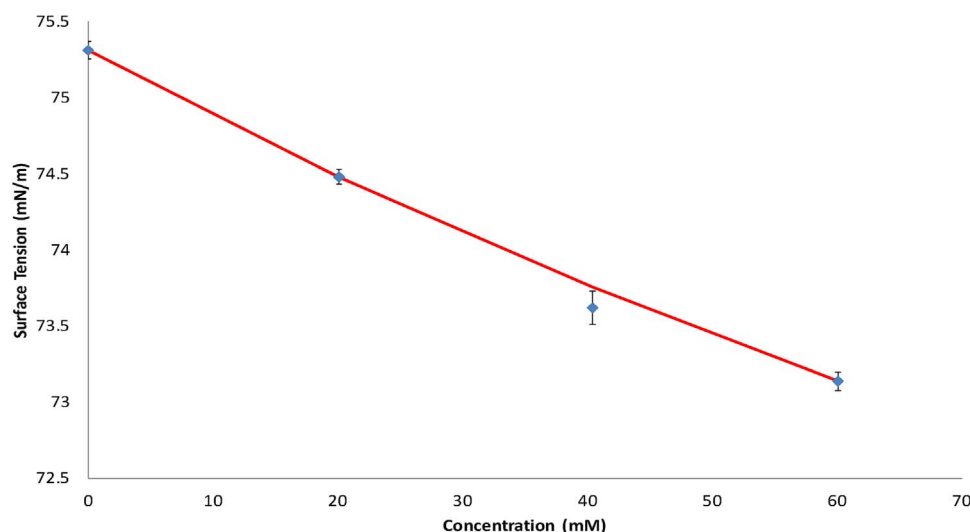


Fig. 5. Experimental (symbols) equilibrium values of the interfacial tension as a function of the amphiphile bulk concentration. Solid line represents the Langmuir-Szyszkowski equation.

Table 1

Values of maximum surface concentration Γ_{\max} and parameter a for the different interfaces.

Solid-Liquid Interface		Gas-Liquid Interface	
Γ_{\max} ($\mu\text{mol}/\text{m}^2$)	a (mol/L)	Γ_{\max} ($\mu\text{mol}/\text{m}^2$)	a (mol/L)
4628	238	2.11	0.12

mN L/m mmol is not an easy interpretation, this is not a concern for this study since the aim is to simply rank the amino acids based on their different hydrophobicity index (H.I.).

Surface tension measurements were carried out by pendant drop method as described in Section 2.5. The surface tension of amino acid solutions with concentration ranging from 0 to 1 M was measured; the results are presented in Fig. 7.

The hydrophobicity index was established from the gradient of the linear section of the surface tension curve, below the critical micelle concentration. Table 2 lists the amino acids and the corresponding hydrophobicity index (expressed in mN L/m mmol); the table also compares the hydrophobicity scale determined in this work with that presented by Bull et al. [27].

With the sole exception of Tyrosine, the two scales are in complete agreement. Bull et al. [27] reported that great difficulty was

encountered during the Tyrosine surface tension measurement and that the slope value was subject to significant error. This could explain the observed difference in Tyrosine position in the hydrophobicity scales.

3.5. Influence of Amino Acids Hydrophobicity on Foam Properties

The amino acids Hydrophobicity Indexes were compared with the maximum foam porosities and the corresponding mean Sauter diameter of foams obtained when the different amino acids were used as amphiphiles. The foam Sauter diameter (d_{32}) was determined using the following equation [28] (Eq. (4)):

$$d_{32} = \frac{\sum (n_i d_i^3)}{\sum (n_i d_i^2)} \quad (4)$$

while the distribution width was expressed by the span value defined as (Eq. (5)) [29]:

$$\text{Span} = \frac{D_{v0.9} - D_{v0.1}}{D_{v0.5}} \quad (5)$$

It has been previously shown that foaming was not observed, under these conditions, when Tyrosine and Alanine were used as amphiphiles. Their low position in the hydrophobicity scale suggests that the low hydrophobicity of the amino acids side chain is not capable of sufficiently reducing the hydrophilicity of titania particles. In addition, since the solubility limit of DL-Leucine was reached before the maximum

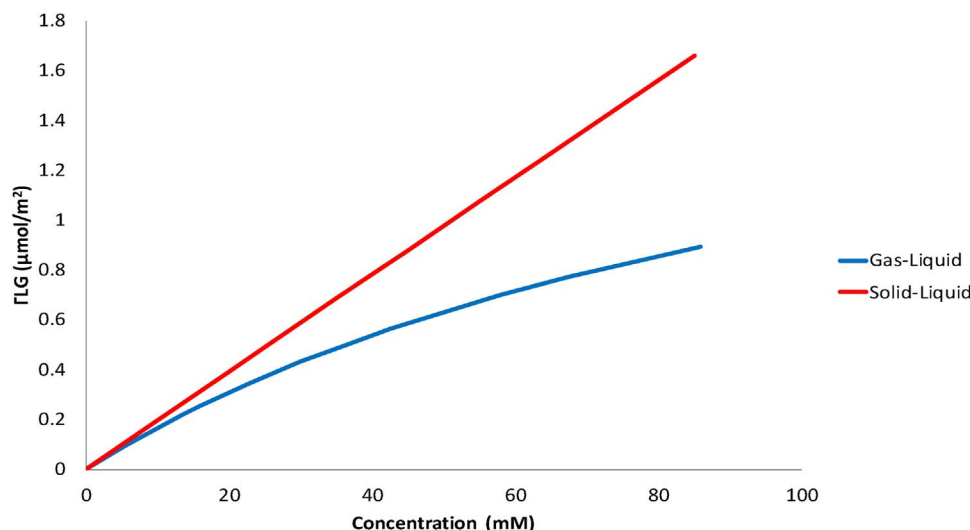


Fig. 6. Comparison of the DL-Phenylalanine isotherms at the Gas-Liquid and Solid-Liquid interfaces.

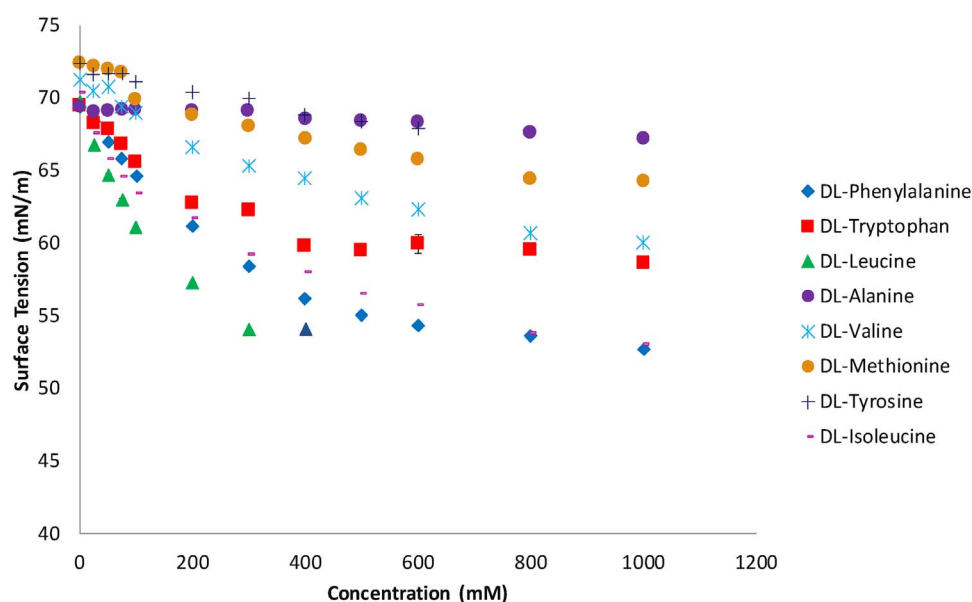


Fig. 7. Surface tension curves for amino acids solutions having different concentrations. The black point in the Leucine curve indicates that the solubility limit for the amino acid was reached.

Table 2
Comparison between the amino acids hydrophobicity scale determined in this work and that proposed by Bull et al.

	Current Work	Bull et al.
Hydrophobicity ↑	Leucine (H.I. = 0.84)	Leucine
	Phenylalanine (H.I. = 0.48)	Phenylalanine
	Isoleucine (H.I. = 0.40)	Isoleucine
	Tryptophan (H.I. = 0.23)	Tyrosine
	Valine (H.I. = 0.21)	Tryptophan
	Methionine (H.I. = 0.12)	Valine
	Tyrosine (H.I. = 0.072)	Methionine
	Alanine (H.I. = 0.020)	Alanine

porosity was observed (Fig. 3), this amino acid is not included in Fig. 8 which shows the porosity and the d_{32} as a function of the amino acids hydrophobicity index.

From Fig. 8 it can be noted that both, the foam porosity and the Sauter diameter, present a monotonic relationship with the amino acid hydrophobicity. The foam porosity increases as the amino acid hydrophobicity increases; the effect of amino acids hydrophobicity on the foam porosity explains the trend observed in Fig. 3 with the maximum foam porosity depending on the type of amino acid used. The opposite trend is observed for the d_{32} where a reduction in bubble size is observed increasing the amino acid hydrophobicity; the distribution span was equal to 1.36, 3.15, 1.56, 2.48 and 2.36 for foams made using Phenylalanine, Isoleucine, Tryptophan, Valine and Methionine respectively as amphiphiles. The effect of particle hydrophobicity on bubble size and foam porosity is extensively reported in the literature. Gonzalez et al. showed that increasing the amphiphile concentration, and consequently the particle hydrophobicity, leads to a reduction in bubble size [13]. In their case the particles hydrophobicity was increased by incrementing the concentration of a given amphiphile with the same effect expected when the particles hydrophobicity is changed varying the nature of the amphiphile. The latter observation is supported by the relationships between foam properties and amino acids hydrophobicity confirming the role of particle hydrophobicity on foam properties and allowing *a priori* selection of the amino acid depending on the desired foam structure.

3.6. Determination of Minimum Amphiphile Concentration

It has been shown in section 3.1 that for the exception of DL-Tyrosine and DL-Alanine all the hydrophobic amino acids gave stable foams. The selection of the ideal amino acid to be used as amphiphile depends on its performances (e.g. possibility of obtaining a good range of porosities), solubility and price. In terms of performances the amino acids that allow to get a wide porosity range are DL-Leucine, DL-Phenylalanine, DL-Isoleucine and DL-Tryptophan. The solubility and the cost of the mentioned amino acids are summarised in Table 3 allowing a direct comparison among them.

Both solubility and prices were obtained from the Sigma-Aldrich website (consulted on September 2016). The solubility values refer to solubility in water; this values were selected because, at industrial scale, foam production is unlikely to be carried out at such an acidic pH. In addition, the solubility rank is not expected to change with pH [30]. From Table 3, it can be seen that Phenylalanine is the amino acid that presents the lower cost and an acceptable solubility; for this reasons Phenylalanine was selected as a model amphiphile to be used in order to have a deeper insight into the foaming process. In particular, it was quantified the minimum amphiphile concentration necessary to observe the attachment of the modified particles at the air-water interface. This value was determined by surface tension measurement of 25% w/w titania suspensions having different amino acid concentrations [31]. Fig. 9 shows the surface tension trend as a function of the DL-Phenylalanine concentration.

The surface tension value is constant below a Phenylalanine concentration somewhere in the range 0.045–0.055 M. After this point the surface tension drops indicating that the modified particles start to attach at the air-water interface. The measurement of the surface tension of titania suspensions having Phenylalanine concentrations higher than 0.065 M was not possible due to the formation of foams that prevented the formation of a drop. The equality of the surface tension values below 0.065 M was assessed by statistical analysis. The *t*-test for unequal variances populations was run on each pair of values [32]. The *t*-test was used to test the null hypothesis that the means of the two populations were equal. In order for the null hypothesis to be true the t_{Stat} value has to be comprised between $-t_{Crit}$ and t_{Crit} ($-t_{Crit} < t_{Stat} < t_{Crit}$); Table 4 summarises the t_{Crit} and the t_{Stat} values for the tested surface tension pairs.

From Table 4 it should be noted that pair N° 5 is the first one to present inequality between the two surface tension values but, from Fig. 9, it can be seen that the error bars for the surface tension values

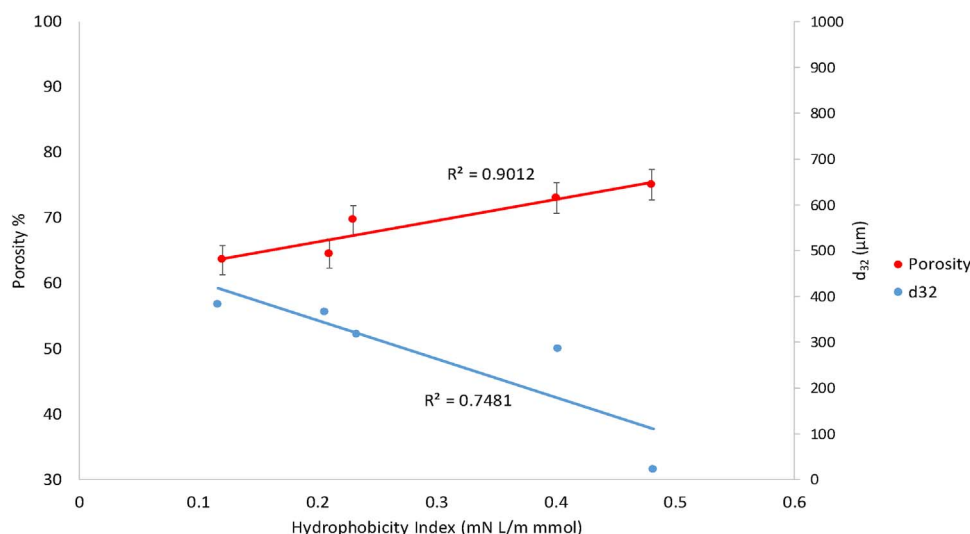


Fig. 8. Maximum foam porosity and d_{32} as a function of the amino acid hydrophobicity index.

Table 3
Comparison of amino acids solubility and cost.

Amino Acid	Solubility (g/L)	Cost (£/100 g)
Leucine	24.3	138.50
Phenylalanine	29.6	39.80
Isoleucine	41.2	154.50
Tryptophan	11.4	171.20

relative to a Phenylalanine concentration of 0.02 M and 0.055 M overlaps. For this reason, the t-test on these two values was carried out and from Table 4 it can be observed that the difference between them is not significant. The surface tension for the 0.065 M suspension was compared to the surface tension values of both the 0.055 M and 0.02 M suspensions. In both cases the difference between the two values was statistically significant indicating that a Phenylalanine concentration of (0.060 ± 0.005) M is the minimum amount that has to be added in order to have the attachment of the modified particles at the air-water interface. It has to be borne in mind that this concentration value is specific for the tested amino acid and the operating conditions. This value is, in fact, affected by the pH of the ceramic suspension, due to the different pK_a values of the amino acids, and by the different

hydrophobicity of the amino acids side chains.

4. Conclusion

Hydrophobic α -amino acids were used as amphiphiles for the production of ceramic foams using the direct foaming technique. This class of amphiphile is more environmentally benign in respect to conventional ones and allows a wider pH operational window. It has been demonstrated that the amino acids adsorb on the particles surface by either the carboxylic or amino group in acidic and basic conditions respectively. In addition, the partition of a model amino acid (e.g. Phenylalanine) between the solid-liquid and gas-liquid interfaces has been determined giving an insight into the distribution of the amino acid among the different interfaces. The tested amino acids have been classified accordingly to the hydrophobicity of their side chain. The amphiphile hydrophobicity index has been related to both the maximum porosity and the bubble size distribution of foams obtained when they are used as amphiphiles. Monotonic relationships have been observed in both cases with the possibility of a linear relationship in the case of porosity. These give a deeper insight into the role of amphiphile structure on the foam properties offering the possibility of tailoring them. Among the tested amino acids DL-Phenylalanine has been identified as the most suitable to be used thanks to its acceptable solubility

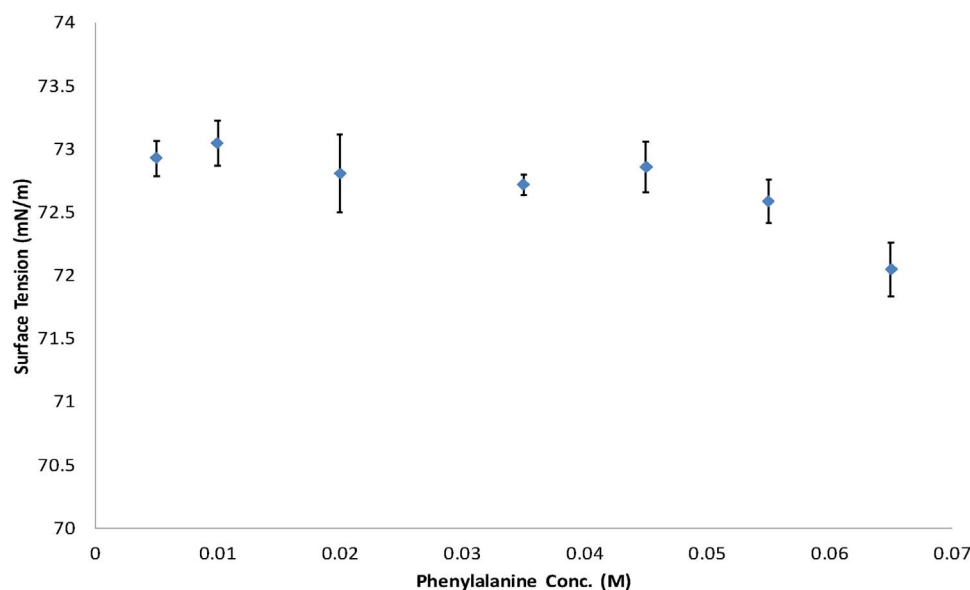


Fig. 9. Surface tension measurement of 25% w/w titania suspension having different phenylalanine concentrations.

Table 4 t_{Crit} and t_{Stat} values for surface tension pairs.

Pair N°	Surface Tension Pairs (mN/m)	t_{Crit}	t_{Stat}	Response
1	72.93 \pm 0.14 (0.005 M)–73.05 \pm 0.18 (0.010 M)	2.31	–1.15	Equal
2	73.05 \pm 0.18 (0.010 M)–72.81 \pm 0.31 (0.020 M)	2.45	1.49	Equal
3	72.81 \pm 0.31 (0.020 M)–72.72 \pm 0.08 (0.035 M)	2.77	2.13	Equal
4	72.72 \pm 0.08 (0.035 M)–72.86 \pm 0.20 (0.045 M)	2.57	–1.49	Equal
5	72.86 \pm 0.20 (0.045 M)–72.59 \pm 0.17 (0.055 M)	2.31	2.35	Not Equal
6	72.59 \pm 0.17 (0.055 M)–72.05 \pm 0.21 (0.065 M)	2.31	4.46	Not Equal
7	72.81 \pm 0.31 (0.020 M)–72.59 \pm 0.17 (0.055 M)	2.45	1.41	Equal
8	72.81 \pm 0.31 (0.020 M)–72.05 \pm 0.21 (0.065 M)	2.36	4.51	Not Equal

and relatively low cost. For this amino acid the minimum amphiphile concentration necessary to have stable foams has been identified, however this value is specific to the tested amino acid since it depends on both pH and amino acid hydrophobicity.

Acknowledgements

We thank Dr Jonathan Bradley for NMR analysis. Acknowledgments to EPSRC and Johnson Matthey PLC for funding.

References

- [1] L.J. Gauckler, M.M. Waeber, C. Contiad, M. Jacobdckliere, Ceramic Foam for Molten-Metal Filtration, *J. Met.* 37 (9) (1985) 47–50.
- [2] P. Colombo, M. Sheffled, Cellular ceramics: structure, Manufacturing, Properties and Applications, Wiley-VCH, Weinheim, 2005.
- [3] A.R. Studart, U.T. Gonzenbach, E. Tervoort, L.J. Gauckler, Processing Routes to Macroporous Ceramics: a Review, *J. Am. Ceram. Soc.* 89 (6) (2006) 1771–1789.
- [4] T. Ota, M. Imaeda, H. Takase, M. Kabayashi, N. Kinoshita, T. Hirashita, H. Miyazaki, Y. Hikichi, Porous Titania Ceramic Prepared by Mimicking Silicified Wood, *J. Am. Ceram. Soc.* 83 (6) (2000) 1521–1523.
- [5] R.A. White, E.W. White, J.V. Weber, Replamineform-New Process for Preparing Porous Ceramic, Metal and Polymer Prosthetic Materials, *Science* 176 (4037) (1972) 922.
- [6] J. Saggio-Woyansky, C.E. Scott, W.P. Minnear, Processing of Porous Ceramics, *Am. Ceram. Soc. Bull.* 71 (11) (1992) 1674–1682.
- [7] J. Luyten, S. Mullens, J. Coymans, A.M. De Wilde, I. Thijs, New Processing Techniques of Ceramic Foams, *Adv. Eng. Mater.* 5 (10) (2008) 715–718.
- [8] R.A. Lopes, A.M. Segadaes, Microstructure, Permeability and Mechanical Behaviour of ceramic Foams, *Mater. Sci. Eng. A-Struct. Mater. Prop. Microstruct. Process.* 209 (1,2) (1996) 149–155.
- [9] H. Kim, C. De Rosa, M. Boaro, J.M. Vohs, R.J. Gorte, Fabrication of Highly Porous Yttria-Stabilized Zirconia by Acid Leaching Nickel from a Nickel-Yttria-Stabilized Zirconia Cement, *J. Am. Ceram. Soc.* 85 (6) (2002) 1473–1476.
- [10] A. Imhof, D.J. Pine, Ordered macroporous Materials by Emulsion Templating, *Nature* 389 (6654) (1997) 948–951.
- [11] U.T. Gonzenbach, A.R. Studart, E. Tervoort, L.J. Gauckler, Stabilization of Foams with Inorganic Colloidal Particles, *Langmuir* 22 (2006) 109383–109388.
- [12] A.R. Studart, R. Libanori, A. Moreno, U.T. Gonzenbach, E. Tervoort, L.J. Gauckler, Unifying Model for the Electrokinetic and Phase Behavior of Aqueous Suspensions Containing Short and Long Amphiphiles, *Langmuir* 27 (2011) 11835–11844.
- [13] U.T. Gonzenbach, A.R. Studart, E. Tervoort, L.J. Gauckler, Tailoring the Microstructure of Particle-Stabilized Wet Foams, *Langmuir* 23 (2007) 1025–1032.
- [14] I. Wagner, H. Musso, New naturally Occurring Amino Acids, *Angew. Chem. Int. Ed. Engl.* 22 (1983) 816–828.
- [15] S.E. Forrester, C.D. Rielly, K.J. Carpenter, Gas-inducing impeller design and performance characteristics, *Chem. Eng. Sci.* 53 (1998) 603–615.
- [16] J. Schindelin, I. Arganda-Carreras, E. Frise, Fiji: an open-source platform for biological-image analysis, *Nature Methods* 9 (7) (2012) 676–682.
- [17] A. Williams, C.P. Garner, J.C.P. Binner, Measuring Pore Diameter Distribution of Gelcast Ceramic Foams from Two-Dimensional Cross Sections, Loughborough's Institutional Repository.
- [18] S.M.I. Saad, Z. policova, A.W. Neumann, Design and Accuracy of Pendant Drop Methods for Surface Tension Measurement, *Colloids and Surfaces A: Physicochem. Eng. Aspects* 384 (2011) 442–452.
- [19] K. Bourikas, C. Kordulis, A. Lycourghiotis, Titanium Dioxide (Anatase and Rutile): Surface Chemistry, Liquid-Solid Interface Chemistry, and Scientific Synthesis of Supported Catalysts, *Chem. Rev.* (2014) 9754–9823.
- [20] H.C. Tseng, C.Y. Lee, W.L. Weng, I.M. Shiah, Solubilities of amino acids in water at various pH value under 298.15 K, *Fluid Phase Equilibria* 285 (2009) 90–95.
- [21] D. Megias-Alguacil, E. Tervoort, C. Cattin, L.J. Gauckler, Contact Angle and Adsorption Behaviour of Carboxylic Acids on α -Al₂O₃, *Journal of Colloid and Interface Science* 353 (2011) 512–518.
- [22] V.B. Fainerman, E.H. Lucassen-Reynders, R. Miller, Adsorption of Surfactant and Proteins at Fluid Interfaces, *Colloids Surfaces A: Physicochem. Eng. Aspects* 143 (1998) 141–165.
- [23] I. Langmuir, The constitution and Fundamental Properties of Solids and Liquids. II. Liquids, *J. Am. Chem. Soc.* 39 (1917) 1848–1906.
- [24] A.V. Makievski, V.B. Fainerman, R. Miller, M. Bree, L. Liggieri, F. Ravera, Determination of Equilibrium Surface tension Values by Extrapolation Via Long Time Extrapolations, *Colloids Surf. A* 122 (1997) 269–273.
- [25] J. Eastoe, J.S. Dalton, Dynamic Surface Tension and Adsorption Mechanisms of Surfactants at the Air-Water Interface, *Adv. Colloid Interface Sci.* 85 (2000) 103–144.
- [26] S.S. Dukhin, G. Kretzschmar, R. Miller, Dynamics of Adsorption at Liquid Interfaces, Elsevier Science, 1995.
- [27] H.B. Bull, K. Breeze, Surface tension of Amino Acids Solutions: a Hydrophobicity Scale of the Amino Acid Residues, *Archives of Biochemistry and Biophysics* 161 (1974) 665–670.
- [28] H.G. Merkus, Particles Size Measurements: Fundamentals, Practise, Quality, Springer, 2009, 2017.
- [29] A guidebook to particle size analysis, Hariba Instruments Inc., Irvine, USA.
- [30] T.E. Needham, The solubility of Amino Acids in Various Solvent Systems, (1970) PhD Thesis.
- [31] U.T. Gonzenbach, A.R. Studart, E. Tervoort, L.J. Gauckler, Ultrastable Particle-Stabilized Foams, *Angew. Chem. Int. Ed.* 45 (2006) 3526–3530.
- [32] B.L. Welch, The generalization of Student's problem when several different population variances are involved, *Biometrika* 34 (1–2) (1947) 28–35.